FABRICATION AND INVESTIGATION OF AL-DOPED ZNO NANORODS FOR LASER-BASED TEMPERATURE SENSOR APPLICATIONS

ATIQAH NABIEHA BINTI AZMI

UNIVERSITI SAINS MALAYSIA

2024

FABRICATION AND INVESTIGATION OF AL-DOPED ZNO NANORODS FOR LASER-BASED TEMPERATURE SENSOR APPLICATIONS

by

ATIQAH NABIEHA BINTI AZMI

Thesis submitted in fulfilment of the requirements
for the degree of
Doctor of Philosophy

May 2024

ACKNOWLEDGEMENT

Alhamdulillah. Praise to Allah. Without His Mercy, I would never finished this research. I would like to express my sincere gratitude to my supervisor, Ts. Dr. Wan Maryam bt Wan Ahmad Kamil for her guidance, comments, sincerity and patience. It was an honour to study under her supervision. Without her continuous encouragement and help, this dissertation would not have been possible. I extend my appreciation to my co-supervisors Assoc. Prof. Ts. Dr. Wan Zakiah bt Wan Ismail and Dr. Mohd Mahadi bin Halim for their support and assistance throughout this journey. This project was funded by Kementerian Pendidikan Malaysia through Fundamental Research Grant Scheme (FRGS) under account number: FRGS/1/2018/STG02/USM/02/6

I also thanked the staff of the nano-optoelectronics research laboratory (NOR Lab) and Department of Photonics, National Cheng Kung University, Taiwan for their technical assistance during my laboratory work. Special thanks to my friends and colleagues who have been with me on this journey, Fadzliana, Abdullah, Tamim, Nurizati, Ainita, Zulfa, Mimi, Puteri, Kevin, Syairah, Hidayah, Syahida, Zuria and Rose. They have made the challenges more manageable and the successes more joyful.

To my husband, Ahmad Helmi bin Mahamarowi and kids Luth and Hawa, thank you for the unconditional love, belief in me, and the countless sacrifices that you have made. Your unwavering support has been my constant motivation. I am also indebted to my parents, siblings and family-in-law for endless help, support and care. Without them, this journey is impossible. Thank you for always one step behind me all the way. Thank you.

TABLE OF CONTENTS

LIST OF TABLES

LIST OF FIGURES

LIST OF SYMBOLS

a	Lattice constant in a-axis for bulk material
c	Lattice constant in c-axis for bulk material
c/a	Ratio for an ideal hexagonal close-packed structure
h	Plank's constant
m_e^*	Effective electron mass
n_e	Electron carrier density in the conduction band
C	Decay time of spontaneous emission
$N_1(t)$	Number of excited molecules
$P(t)$	Pump rate
$q(t)$	Number of photons in laser modes
τ	Cavity-decay time
$D(\lambda)$	The diffusion constant of light
$l_t(\lambda)$	Static transport mean free path
j_n's	Spherical Bessel functions of the first kind
h_n's	Hankel functions
μ_1, μ_2	Magnetic permeability of the sphere and surrounding medium
$\langle cos\ \theta \rangle$	Average cosine of the scattering angle obtained from the differential scattering cross-section.
l_t	Transport mean free path
l_s	Scattering mean path
Ro	The intensity ratio at room temperature from the graph of the linear function intensity ratio of the signals against temperature
D	Crystallite size
k	Constant of 0.94
λ	Wavelength of X-ray
B, ω, $\Delta\lambda$	Full width at half maximum
θ	Bragg's angle
d	Interplanar spacing
h, k, l	Miller indices
ε	Lattice strain
δ	Dislocation density
$F(R)$	Ratio of the absorption coefficient to the scattering coefficient
E_g, ΔE	Band gap energy
hv	Incident photon energy
$\lambda peak$	Wavelength of random laser peak
k	Boltzmann constant
T	Temperature

D^O	Neutral donors
D^+	Ionized donors

LIST OF ABBREVIATIONS

Al	Aluminium
Al_2O_3	Aluminium oxide
AFM	Atomic Force Microscopy
B	Boron
C	Carbon
CB	Conduction Band
CBD	Chemical Bath Deposition
CO_2	Carbon Dioxide
CVD	Chemical Vapor Deposition
CVT	Chemical Vapor Transport
DFG	Difference Frequency Generation
DLE	Deep Level Emission
EDX	Energy Dispersive X-Ray
FESEM	Field Emission Scanning Electron Microscopy
FWHM	Full Width at Half Maximum
H_2	Hydrogen Gas
H_2S	Hydrogen Sulfide
HCHO	Formaldehyde
HMT	Hexamethylenetetramine
Ga	Gallium
GaAs	Gallium Arsenide
ICSD	Inorganic Crystal Structure Database
K-M	Kubelka-Munk
LED	Light Emitting Diode
LIDAR	Light Detection And Ranging
LMS	Laser Measurement System
MIG	Metal Inert Gas
MOCVD	Metal-Organic Chemical Vapor Deposition
MOVPE	Metal-Organic Vapor-Phase-Epitaxy
N	Nitrogen
NaCl	Sodium Chloride
NH_3	Ammonia
NO_2	Nitrogen Gas
NBE	Near Band Edge
NR	Nanorod
O	Oxygen
OPO	Optical Parametric Oscillator
OSNR	Optical Signal To Noise Ratio

PL	Photoluminescence
PSPD	Position-Sensitive Photo Detector
PVP	Polyvinylpyrrolidone
RF	Radio Frequency
RL	Random Laser
SiO_2	Silicon Oxide
SnO_2	Stannic Oxide
SO_2	Sulphur Oxide
UV	Ultraviolet
UV-Vis	Ultraviolet-Visible
VB	Valence Band
VLS	Vapor-Liquid-Solid
XRD	X-Ray Diffraction
ZnO	Zinc Oxide

FABRIKASI DAN KAJIAN NANOROD ZNO TERDOP AL UNTUK APLIKASI PENGESAN SUHU BERASASKAN LASER

ABSTRAK

Kajian ini mengetengahkan potensi laser rawak sebagai pengesan haba berasaskan laser pada suhu bilik dalam julat UV. Kaian termasuk sintesis dan pendopan nanorod ZnO serta mengukur parameter laser dan pengesan berasaskan laser. Nanorod ZnO disintesis pada substrat kaca menggunakan kaedah pemendapan rendaman kimia (CBD) selama tiga jam pada 96 ° C menunjukkan purata ketinggian nanorod dan diameter ialah masing-masing 1200 nm dan 176 nm. Dopan Al kemudiannya diperkenalkan kepada nanorod ZnO menggunakan teknik celupan. Pada mulanya, kepekatan dopan Al dalam julat luas (10 mM - 70 mM) pada tempoh celupan yang ditetapkan pada 100 saat disiasat. Didapati purata ketinggian nanorod ZnO berkurangan dengan peningkatan kepekatan Al disebabkan keasidan larutan dopan. Hasilnya, hanya ZnO yang didop dengan kepekatan 10 mM menunjukkan pancaran laser rawak dengan nilai ambang 17.83 mJ/cm^2 dan lebar spektrum 1.66 nm. Berdasarkan hasil ini, tempoh didop (0 hingga 80 saat) diubah pada kepekatan yang sama iaitu 10 mM. Terdapat peningkatan Al % dan purata diameter nanorod ZnO tidak berubah dengan peningkatan tempoh (± 14 nm). Semua sampel menghasilkan pancaran laser rawak dan nanorod ZnO yang didop 40 saat dengan 1.19 % Al menunjukkan nilai ambang terendah 12.48 mJ/cm^2 dengan lebar spektrum 1.76 nm. Akhirnya, pengesan haba berasaskan laser disiasat. Nanorod ZnO yang didop 60 saat menunjukkan sensitiviti serendah 0.001 C^{-1}. Kesimpulannya, ZnO didop 40 saat menunjukkan ambang laser rawak terbaik dan ZnO yang didop 60 saat memberi

pengesan terbaik kerana lebar spektrum yang kecil. Kajian ini menunjukkan nanorod ZnO didop Al boleh dijadikan laser rawak dan pengesan haba berasaskan laser.

FABRICATION AND INVESTIGATION OF AL-DOPED ZNO NANORODS FOR LASER-BASED TEMPERATURE SENSOR APPLICATIONS

ABSTRACT

This work highlights the potential of random lasers as thermal laser-based sensor at room temperature within the UV-range. The work includes synthesis of ZnO nanorods, doping the ZnO, measuring the lasing, and laser-based sensing parameters. The ZnO nanorods were synthesized on glass substrate using chemical bath deposition (CBD) method for three hours at 96 °C and revealed an average nanorod height and diameter of 1200 nm and 176 nm, respectively. Al dopant is then introduced to the ZnO nanorods by dipping technique. To start, a broad range of Al dopant concentrations (10 mM - 70 mM) at fixed doping duration of 100 s was investigated. The average height of ZnO nanorods decreased with increasing concentration of Al due to the acidity of the doping solution. As a result, only ZnO doped with 10 mM concentration showed random lasing emission at a threshold of 17.83 mJ/cm^2 with a spectral width of 1.66 nm. Based on these results, doping duration (0 s to 80 s) was varied for a fixed concentration of 10 mM. A gradual increase of Al % was observed and the average ZnO nanorods diameter did not change significantly with increasing doping duration (± 14 nm). All samples showed random lasing emission and ZnO nanorods doped for 40 s with 1.19 % of Al showed lowest lasing threshold of 12.48 mJ/cm^2 with a spectral width of 1.76 nm. Finally, thermal laser nano-sensing were investigated. ZnO nanorods doped for 60 s revealed a sensitivity as low as 0.001 C^{-1}. In conclusion, ZnO doped for 40 s showed the best random lasing threshold and ZnO doped for 60 s showed the best sensing properties due to a narrower linewidth. This

work showed that the Al-doped ZnO nanorods is a promising candidate for random lasing and its application as a laser-based thermal nano-sensor.

CHAPTER 1

INTRODUCTION

1.1 Introduction to Laser

Laser is defined as light amplification by stimulated emission of radiation. A conventional laser consists of three important elements to generate the laser emission such as pump energy, gain medium and optical cavity. The laser can be classified based on their gain medium which are gas laser, solid-state laser, fiber laser, liquid laser (dye laser) and semiconductor laser [1]. Laser offers the advantage of a high level of accuracy, ease of automation, and environmentally friendly, especially in laser cutting applications [2]. Owing to special properties of lasers such as highly monochromatic, coherent and collimated, lasers have been applied in a wide range of modern scientific fields including medicine, data storage, communication, and military. As a result, lasers and their potential become an area of interest for the scientific and non-scientific communities.

A random laser (RL) can be classified as a semiconductor laser if it uses a semiconductor material as its gain medium. In this work specifically, the gain medium is II-VI semiconductor material; zinc oxide (ZnO). A random laser is a laser that is different to conventional lasers as the laser emission is generated without an external cavity or also known as an open cavity type of laser. Lasing is achieved by trapping the intended light using nanostructures (by manipulating a change of refractive index). Light trapping in random lasers is achieved through multiple photons scattering processes. Scattering is a phenomenon where the particle absorbs light energy and

causes the particle's motion to change due to collision with another particle. By making the light scatter internally (through the change in refractive index) within an area of the gain medium, it is possible to have gain achieved by the photons scattering. If the photons get to be build up within this area, they can achieve the threshold or lasing and lasing emission is then observed with wavelengths of the gain profile. For example, zinc oxide generally emits spontaneous emission between 375 nm and 395 nm. Hence, it is expected that random lasing will occur within this range for zinc oxide.

The chronology of discovering a random laser started by replacing one of the laser mirrors in a Fabry-Perot cavity with a scattering medium [3]. Letokhov then modified the diffusion theory to introduce scattering by investigating the random walk of photons in a random system to theoretically prove random lasing emission [4]. Lawandy then discovered a multimode laser spectrum without an external cavity - showing the first working principle of a random laser [5].

1.2 Introduction to Zinc Oxide and Al-doped ZnO

ZnO can be synthesized in a variety of nanostructures such as nanowires, nanoflower, nanosheet, nanofiber, and nano forest [6], [7], [8], [9], [10] which lead to various applications. Many synthesis methods are used for synthesizing ZnO nanostructures such as vapour-liquid-solid, chemical vapour transport, thermal chemical vapour deposition, metal-organic vapour-phase-epitaxy, metal-organic chemical vapour deposition, electrodeposition, and sol-gel [11], [12], [13], [14], [15], [16]. However, all these methods include complex processes, high operating temperatures and toxic chemicals. Thus, the chemical bath deposition (CBD)

technique which is simple, easy to handle and requires low operating temperature is an alternative to solve this problem. This method was chosen to synthesize the ZnO nanorods in this work.

Among the semiconductor material used, ZnO is the most stand-out material to act as a scatterer and gain medium in a random laser due to its high exciton binding energy (60 meV), which can produce efficient excitonic emission at room temperature. In addition, it has a high gain (300 cm^{-1}), large saturation velocity (3.2 x 10^7 cms^{-1}), high breakdown voltage, high refractive index, and stability. It is also a promising material for random laser in the UV range due to its wide bandgap energy (3.37 eV). Nowadays, developing short-wavelength emitters based on wide band-gap semiconductors has led to the choice of using ZnO nanostructure in the field of photonics and optoelectronics.

Metal-doped ZnO nanorods have attracted many attentions due to improvement in their electrical, structural and optical properties upon doping. Doping is the process of incorporating specific impurities (dopants) to a semiconductor [17]. It is a critical approach for improving and tuning the crystal structure and optical properties of ZnO nanostructures. Among group III element, Al-doped ZnO nanorod exhibits dense arrays, small nanorods diameter, high porous surface, higher conductivity and superior sensitivity in sensing compared to undoped ZnO [18]. As the objective is to produce high sensitivity sensor, Al dopant was chosen to be doped with ZnO.

1.3 Introduction to Laser-based Sensing

The first laser was built by Theodore Maiman in 1960 based on theoretical work by Charles H. Townes and Arthur Leonard Schawlow [19]. It continues to expand until today as it has low maintenance, high accuracy, and high sensitivity. The laser-based sensing is a device that emits a laser beam to a sample and receives the reflected light. It can detect any changes in the sample. The laser-based sensing can be categorized as destructive and nondestructive, depending on the purpose of the investigation.

Destructive techniques alter or irreversibly damage the sample during the sensing process. This alteration may involve physical removal of material, changes to the sample's structure, or chemical reactions induced by the laser. Destructive methods are often used when sample destruction is acceptable or when detailed analysis requires sample preparation. For example, laser ablation, laser cutting, laser drilling, and laser-induced damage testing [20], [21], [22].

Meanwhile, non-destructive techniques analyze the sample without causing permanent changes or damage. These methods are preferred when preserving the integrity of the sample is essential or when repeated measurements are necessary. Non-destructive sensing allows for detailed analysis while keeping the sample intact such as laser Raman spectroscopy, laser interferometry, and laser speckle imaging [23], [24], [25].

The commonly used optical sensor is fluorescence-based which has low signal amplification due to its broad emission line, low signal-to-noise ratio, the absence of nonlinearity, and low sensitivity compared to the laser-based sensor [26]. All the

weaknesses of the fluorescence-based sensor can be solved by laser-based sensing which offers higher signal amplification and higher signal-to-noise ratio due to narrow emission lines as well as high sensitivity due to nonlinear components.

Therefore, in this study, random lasing emission generated by Al-doped ZnO will be investigated to act as a nano-thermal sensor. An example of a nano-thermal sensor is a luminescent nanothermometer whereby nanoparticles that have luminescence with strong thermal dependence can be used to determine actual nanoparticle temperature. The main advantage of luminescent nanothermometers is the capability to remotely probe the temperature of a system without any physical contact [27], [28], [29]. The random lasing has emerged as a potential laser-based sensor since they are extremely sensitive to even the smallest variations in temperature fluctuations; an ideal option for use as nanothermometers in probing temperature variations within nanostructure systems [30], [31], [32].

Random lasers have the added advantage of manipulating scattering to induce lasing. Therefore, changes in the scattering properties, for example, changes in cell structure, will change the lasing characteristics. As such, changes in biological analytes such as microorganisms, cells, biomolecules, and other biological structures can correspondingly be detected [33]. This makes random lasers one of the promising candidates for biosensor applications. There are many types of biosensors such as piezoelectric, thermal, enzyme-based, tissue-based, and immune sensors which are used for different applications. For example, biosensors can be used to detect bacteria and pathogens such as Escherichia coli (E. coli) [34].

Thus, this study will focus on the investigation of generating the random lasing emission by Al-doped ZnO to act as a nano-thermal sensor. The goal is to improve the

RL emission in terms of lowering the threshold power, increasing lasing intensity, narrowing line width, producing a high Q-factor value and proving the capability of a random laser to become a nano thermal sensor.

1.4 Problem Statement

Random lasers have been employed in numerous biosensor applications to detect cancerous thyroid, changes in structure and composition of brain tissues, small pH and temperature variations, uterine tissues, omit low levels of dopamine, and to distinguish malignant and healthy tissues [32], [35], [36], [37], [38], [39], [40]. However, lowering the lasing thresholds for advancing in this field is still a challenge. Numerous initiatives to lower the lasing thresholds include using dye-doped polymer films [41], [42], [43], altering the irradiated laser conditions [44], coupling the random cavity modes with planar microcavity modes [45], employing SnO_2 nanowires coated with an amorphous layer [46], doping of Al [47], doping of gold [48], and employing a SiO_2 capping layer with ZnO nanorods [49]. But still, the lasing threshold value is higher.

It has been demonstrated that doping ZnO with Al can reduce resistivity, increase transmittance in the visible area, obtain high conductivity, provide high sensitivity, generate extra electrons, and increase the band gap energy [50], [51], [52]. Doping with Al was also reported to enhance photodetector performance in terms of long-term emission current stability, fast response and recovery time, and better electrical conductivity compared to pure ZnO [53], [54], [55]. The Al is also a non-toxic, low-cost dopant solution, and has low energy consumption. These advantages

make Al the ideal choice for doping with ZnO. In addition, Al is the most common doping element used in solution-based growth techniques to dope ZnO [56], [57], [58]. Al is known to be a suitable material to dope with ZnO as it has a small ionic radius (0.53 Å) to interstitially substitute or interstitially combine with Zn ions (0.74 Å) in the ZnO nanostructures [59]. As such, testing this theory of doping with Al for random lasing can help solve this problem of lowering the lasing threshold.

However, the current method of doping with Al for random lasers has limitations. Current methods employ in-situ doping techniques whereby the Al dopant is introduced during the synthesis or growth of ZnO nanorods. A challenge that arises when employing the in-situ method of doping is doping may change the growth mechanism of ZnO nanorods. For example, the ZnO nanorods were observed to transform into ZnO nanoplates when Al content was above 5 % [60]. Doping that changes morphology hinders the possibility of utilizing doped nanostructures for optoelectronic devices. Other than that, in-situ doping causes a slower growth rate during CBD due to the presence of $Al(OH)^{4-}$ when the Al dopant is increasing [59]. The previous work on in-situ doping of Al revealed that it is still a challenge to increase the doping percentage for ZnO nanorods whereby the maximum reported limit of doping concentrations was between 0.67% [47] and 1.72% [61]. To solve the problems associated with in-situ doping, this work proposes simple ex-situ doping of ZnO nanostructure to increase the doping concentration in ZnO whereby doping is introduced after the synthesis of ZnO.

ZnO was reported in its ability to be a gas sensor, chemical sensor, biosensor, fluid sensor, UV sensor, humidity sensor, mass sensor and nano-force sensor [62], [63], [64]. Improvement of selectivity and sensitivity was further achieved by

employing ZnO with dopants such as aluminium, cobalt, gallium, and copper (II) oxide [65], [66], [67]. The problem with the prior ZnO-based sensor was that it required high power consumption to run and could only run well at high temperatures of 300 °C - 500 °C [68], [69]. To solve the problem of high working temperature for ZnO-based sensors and the need for UV-based laser-sensing, we prepared Al-doped ZnO nanorods to act as a random laser-based nanothermometer working at room temperature. As random lasers are sensitive to small changes within the nanostructure system, a small increase in system temperature changes the properties of the random laser.

Laser-based sensing has been suggested for small-area sensing as lasers have high signal amplification, low signal-to-noise ratio due to narrow emission lines, and high sensitivity due to nonlinearity [70], [71], [72]. The random laser has emerged as a potential laser-based sensor since they are extremely sensitive to even the smallest variations in temperature fluctuations; an ideal option for use as nanothermometers in probing temperature variations within nanostructure systems [32], [73], [74]. Sensing in biological systems with UV range optical excitation is desirable as one of the major biological entities such as nucleic acids which can absorb UV light strongly, permitting their sensitive quantification [75], [76], [77]. However, no UV-based random laser-based sensing is known to date. This work aims at providing a proof of concept that an Al-doped ZnO-based random laser is a promising candidate for biosensors and nanothermometers within the biological system.

1.5 Objective of the Study

The main objectives are outlined as below:

1. To characterize the effect of ex-situ doping of Al on the structural and optical properties of the ZnO nanorods synthesized by the CBD method.
2. To investigate random laser emission properties; threshold, line width and Q-factor.
3. To demonstrate laser-based thermal sensing from Al-doped ZnO at room temperature in UV region.

1.6 Originality of the Study

The originality of the study is based on the following points:

1. No previous report on the ex-situ doping dip method for Al-doped ZnO nanorods for random lasing.
2. Previous works of Al-doped ZnO nanorods have a limitation of 1 % of Al concentration as the doping method was in-situ. This study aims to provide novelty in creating Al doping with higher than 1 %.
3. No previous reports about Al-doped ZnO as a laser-based thermal sensor to date.

1.7 Thesis Outline

This thesis is divided into several chapters, based on the following:

Chapter 1 highlights the introduction to the research work within the context of this thesis, the problem statement, objectives, originality and thesis outline.

Chapter 2 provides the literature review and theoretical background of ZnO, a review of methods used to synthesize ZnO nanostructure, a review of metal-doped ZnO, the concept of random laser and different types of sensors utilizing ZnO and laser-based sensors.

Chapter 3 describes the methodology and the equipment used in this work. The type of characterizations and the basic working principle of the equipment used are also explained.

Chapter 4 discusses the results obtained from this work. The morphological, structural, and optical characterizations of the Al-doped ZnO NRs are presented here. This is followed by detailed discussion on RL results and sensor results.

Chapter 5 provides the conclusion and suggestions for future works.

CHAPTER 2

LITERATURE REVIEW

2.1 Introduction

This chapter reviews the characteristic and properties of ZnO including its crystal structure, surface, morphology and optical properties. It is then followed by an overview of the methods used to synthesis ZnO nanostructure, including the CBD method, which was employed in this work. Afterwards, the review of metal doped ZnO and effect of Al doping on both morphology and optical properties were reviewed. Additionally, a review of the random laser's concept, gain medium and scatterer, incoherent and coherent, and improvement to the lasing threshold, were reviewed. Next, this chapter reviews the numerous types of laser-based sensing, including remote sensing, RL biosensors, and RL for disease diagnosis. Lastly, the sensitivity of laser-based sensing was highlighted.

2.2 Properties of ZnO

ZnO is classified as a semiconductor in group II-VI, whose covalence is on the boundary between ionic and covalent semiconductors. As it is an inorganic compound, it is used in the manufacturing processes and can be found in rubbers, plastics, ceramics, glass and cement. The ZnO is an n-type semiconductor material due to the presence of oxygen vacancies in the ZnO lattice. Owing to the wide band gap of the ZnO (3.37 eV), it shows potential to be applied in the ultraviolet (UV) range for high

voltage, high frequency and high power device. In addition, a high exciton binding energy of 60 meV allows significant excitonic emission to be produced at room temperature. ZnO has a high sensitivity to the surface which is why it is really sensitive to the exposure of the surface of various gases such as nitrogen oxide (NO_2), ammonia (NH_3), acetone, hydrogen (H_2), hydrogen sulfide (H_2S), carbon dioxide (CO_2), and sulfur oxide (SO_2) [78], [79], [80], [81], [82], [83], [84] . Other than that, ZnO also shown its capability to become humidity sensor, chemical biosensor and pressure sensor [85], [86], [87]. The physical properties of ZnO are listed in Table 2.1.

Table 2.1: Properties of ZnO [88], [89].

Physical parameters	**Value**
Molecular formula	ZnO
Molar mass	81.408 g/mol
Colour	Milky white solid (cold), yellow solid (heat)
Odor	Odorless
Solubility in water	0.16 mg/ 100 mL (30 C)
Density	5.606 g cm^3
Stable phase at 300K	Wurtzite
Melting point	1975˚C
Boiling point	2360 °C
Thermal conductivity	0.6
Static dielectric constant	8.656
Refractive index	2.008
Energy gap	3.37 eV, direct
Exciton binding energy	60 meV
Electron effective mass	0.24
Hole effective mass	0.59
Electron Hall mobility at 300 K for low n-type conductivity	200 cm^2/V.s
Hole Hall mobility at 300 K for low p-type conductivity	5-50 cm^2/V.s
Structure	Hexagonal,a=b≠c
Lattice energy	964 kcal/mole
Piezoelectric coefficient	12 pC/N
Pyroelectric constant	6.8 A/s/cm^2/K x 10^{10}
Standard enthalpy of formation	-348 kJ/mol

Lattice parameter at 300 K a c c/a	 0.3269 nm 0.5207 nm 1.60

2.2.1 Crystal Structure of ZnO

Figure 2.1 shows the cubic rocksalt, zinc blende, and wurtzite crystal structures of ZnO. The wurtzite crystal structure of ZnO has the highest crystallinity and is the most thermodynamically stable among the three crystal structures. As ZnO exists in the wurtzite crystal structure, Zn cation and O anion bond together in a tetrahedral geometry. This means that each Zn cation is surrounded by four O anions at the corner of the tetrahedral and each O anion is surrounded by four Zn cations.

The hexagonal wurtzite structure of ZnO consists of two lattice parameters, *a* and *c* as shown in Figure 2.2. The values of a and c in ambient conditions are 0.32469 nm and 0.52069 nm, respectively. The ratio of c/a for an ideal hexagonal wurtzite is 1.633 [90], while for ZnO hexagonal wurtzite value is between 1.593-1.603 [91]. The difference in lattice parameters can be affected by excess free carriers, high concentration of point and extended defects and external stresses [92].

While the cubic rocksalt (NaCl) form can only be attained at high pressure, which is approximately at 10 GPa [91], the cubic zincblende structure can only grow on a substrate with a cubic lattice structure and maintain its stability. This is because high pressure may result in a decrease in the lattice parameters, which in turn leads to a preference for ionic rather than covalent behaviour in the bonding between the Zn

ion and O ion [91].

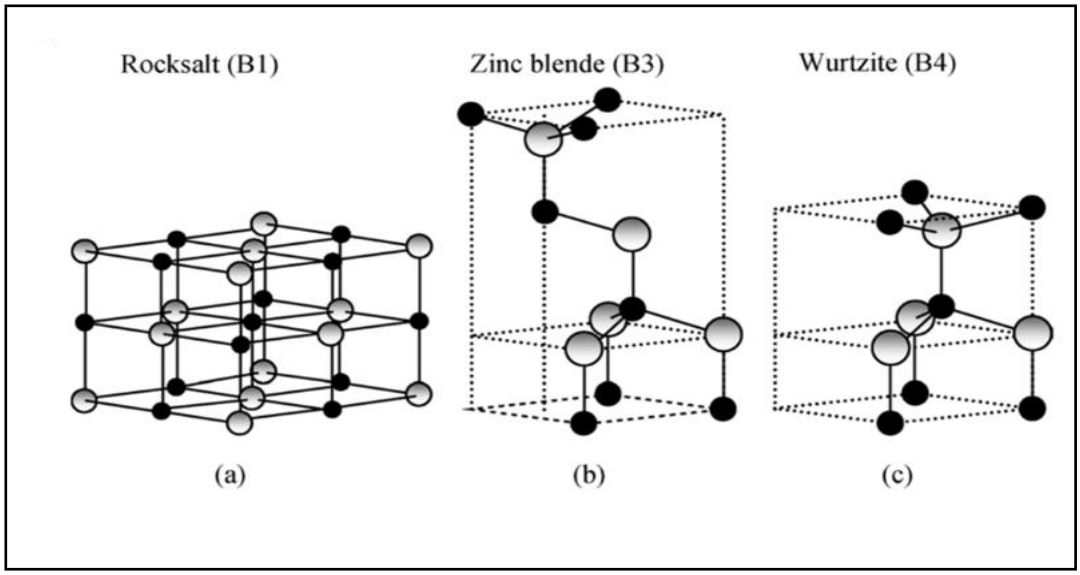

Figure 2.1: ZnO crystal structures: (a) cubic rocksalt (B1), (b) zinc blende (B3), and (c) wurtzite (B4). Grey and black spheres are Zn and O atoms, respectively [91].

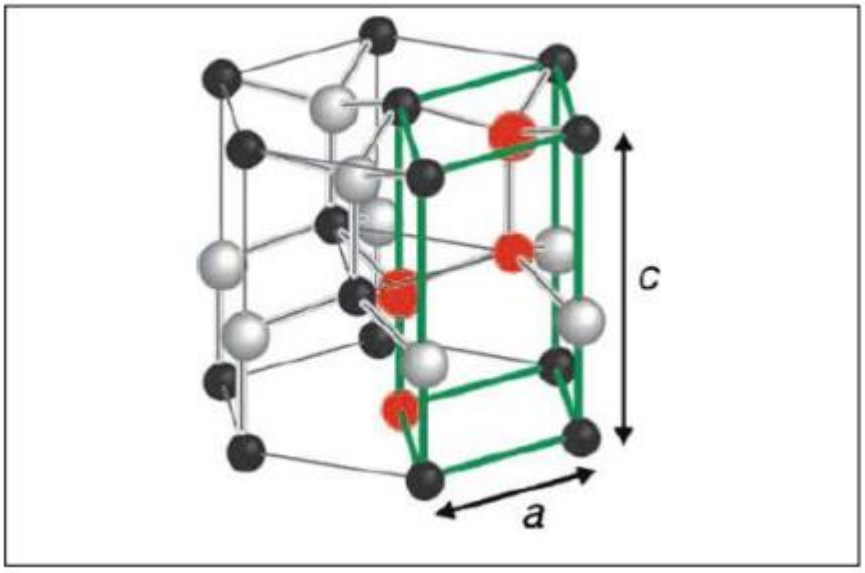

Figure 2.2: Hexagonal wurtzite structure of ZnO with lattice parameters [93].

2.2.2 Surface of ZnO

The hexagonal wurtzite structure of ZnO consists of two polar surfaces and six non-polar surfaces [94] as shown in Figure 2.3. The two polar surfaces are the Zn-polar face (0001) and the O-polar face ($000\bar{1}$). The Zn-polar surface is a positively charged surface while the O-polar surface is a negatively charged surface. Both surfaces have their own polarity because only a single type of terminated atom resides on the surface [95]. As for the six non-polar surfaces, they have no dipole because the surface contains the same amount of Zn and O atoms. The (0001) Zn terminate face has a dipole moment pointing outward while the ($000\bar{1}$) O terminate face has a dipole moment pointing inward [96]. It was reported the polar surface has higher surface energy and a more active surface than the nonpolar surface [97]. Based on work in [96], methanol, water, formic acid, and formaldehyde were absorbed onto the surfaces of ZnO. This is due to high surface to volume ratio hence ZnO can act as a gas sensor. It also reported the ZnO's surface polarity could influence the morphology of the nanostructure grown [98].

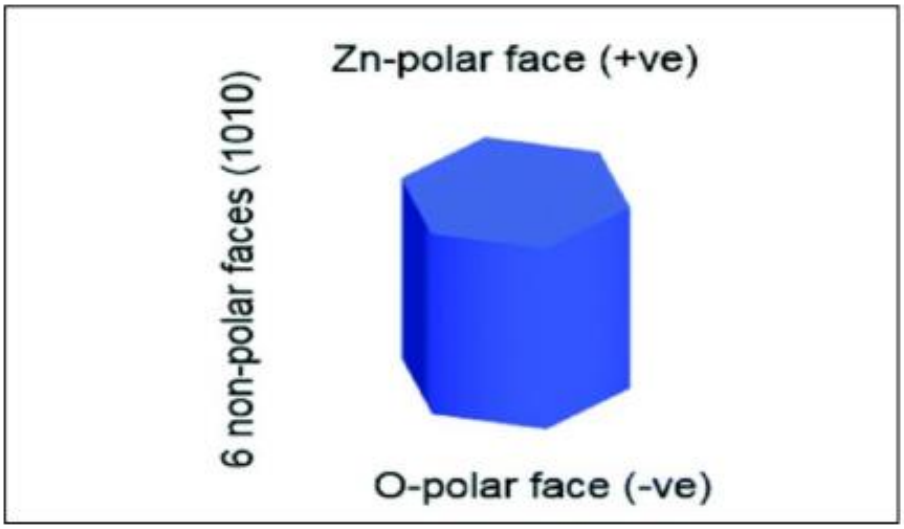

Figure 2.3: Polar and nonpolar faces of ZnO along c-axis [94].

2.2.3 Morphology of ZnO

ZnO nanostructures have been synthesized in many morphologies, such as nanorods, nanowire, nanofiber, nanosheet, nanoflower, nanoneedles, and thin film. It can be approached in many ways such as CBD, atomic layer deposition, sol-gel, chemical vapor deposition, and vapor solid deposition. Different morphology leads to various applications. The ZnO becomes the interest of the researcher as it can applicability to wide-scale application. Different morphology of ZnO using different techniques leading to various applications are listed in Table 2.2 below.

Table 2.2: Various morphology of ZnO prepared by different methods with its applications.

Year	Morphology	Method	Application	Ref
2023	nanowires	CBD	Characterization investigation	[99]
2022	thin film	CVD	Waveguide sensor	[100]
2021	nanowalls	CBD	Random laser	[101]
2020	nanorods	CBD	Random laser	[47]
2019	nanorods	CBD	Laser	[102]
2017	nanorods	CBD	Nanophotonic device	[103]
2017	nanorods	CBD	Random laser	[104]
2016	nanorods	CBD	Photonic device	[105]
2016	nanowire	Atomic layer deposition	Stabilize the PL emission	[6]
2016	nanowire	CBD	Nanoscale device	[106]
2016	nanorods	CBD	Characterization investigation	[107]
2016	fibers, nanorods, cauliflowers, nanorod balls, nanoforest, nanopencils, ellipsoids, nanotubes	CBD	Characterization investigation	[108]

2016	nanofibers	CBD	UV photodetector	[9]
2016	nanorods	Hydrothermal	Random laser	[44]
2016	1D nanorods, 2D nanosheets, 3D double-sided comb-like	Hydrothermal	Solar cells, photocatalysts and nanodevices	[109]
2015	nanoflower	Thermal decomposition	Gas sensing and photocatalysis	[7]
2015	nanorods	Combination of CBD and rapid thermal	Display technology for high-brightness applications	[110]
2015	nanorods	CBD	Photovoltaic device	[111]
2015	nanorods	CBD	Light sensors	[64]
2015	nanorods	CBD	Characterization investigation	[112]
2014	nanorods	CBD	Chemical sensor, photovoltaic, photocatalysis	[113]
2014	nanorods	Sol-gel	Optoelectronic	[114]
2014	nanorods	CBD	Characterization investigation	[115]
2012	thin film	Hydrothermal	Fluid sensor	[63]
2011	nanosheet	Solvo-thermal	Device with a high energy surface, nanoreactors, sensors, nanoscale optoelectronics and solar cell	[8]
2011	nanorods	Atomic layer deposition	Semiconductor-polymer solar cells	[116]
2011	nanorods	Hydrothermal	Polymer solar cell	[117]
2010	nanorods	CBD	Optoelectronic nano device	[118]
2010	nanorods with a cone	Hydrothermal	Treatment of organic pollutants	[119]
2010	thin film	Sol-gel	Optoelectronic and gas sensing	[120]
2010	nanoforest	Chemical-vapor deposition	Solar cell	[10]
2009	nanorods	Hydrothermal	Random laser	[41]
2009	nanorods	CBD	Nanodevice	[121]
2009	nanorods	Hydrothermal	Nanorods-based device	[122]
2007	nanorods	CBD	Optoelectronic device	[123]

2007	nanorods	CBD	Polymers	[124]
2007	thin film	Combination of sol-gel and CBD	Electronics	[125]
2007	nanorod arrays	Metal-organic vapour phase epitaxy	LED	[126]
2007	nanowires	Gold-catalyzed vapor transport	Recyclable photocatalysts	[127]
2007	nanorods	Chemical method in aqueous solution	Photovoltaic	[128]
2006	nanoneedles	Ion-beam	UV random laser	[129]
2006	nanowire	Vapor-solid	Photonic device	[130]
2005	films	CBD	Characterization investigation	[131]
2005	nanosheets	CBD	UV light source	[132]
2004	film	Plasma-enhanced chemical vapor deposition	Random laser	[133]
2004	thin film	Filtered cathodic vacuum arc	Random laser	[134]
2003	nanoparticle	Spray pyrolysis	Characterization investigation	[135]

2.2.4 Optical Properties of ZnO

Both intrinsic and extrinsic effects the optical properties of a semiconductor [136], [137]. For intrinsic, the optical transition occurs between the electrons and holes in the conduction and valence bands. It occurs when an excitonic effect exists from Coulomb interaction. Meanwhile, the optical transition for extrinsic is related to the localized electronic states generated in the bandgap by dopants/impurities or point defects and complexes. Hence, it affects processes of emission and optical absorption. Excitons are classified into free and bound excitons [138], [139], [140]. Bound excitons are those excitons that are bound to the neutral or charged donors and

acceptors. There is a strong dependence of electronic states of bound excitons on the semiconductor material, particularly the band structure.

Thomas explored the basics of absorption edges and exciton structure of ZnO [138]. The properties and applications of ZnO nanostructure invite researcher's interest to implement it in the manufacturing of optoelectronics due to its direct wide band gap (3.37 eV) under ambient conditions, considerable exciton binding energy (60 meV) and efficient radiation recombination. The wide direct band gap of ZnO implies that it covers both blue-UV emission and large exciton binding energy which enables effective excitonic emission at low excitation energy under ambient conditions.

The optical properties of ZnO such as absorption, transmission, reflection, photoluminescence (PL), photo reflection, spectroscopic ellipsometry, cathodoluminescence and calorimetric spectroscopy have been explored. However, in this thesis, we focused on photoluminescence. The properties of semiconductors can be subjected to changes to produce the 'quantum confinement effects' when minimized the bulk exciton Bohr radius to the 2.34 nm size [141]. Based on photoluminescence data, quantum confinement can increase the energy band gap of ZnO [142], [143]. PL is generated by the radiative recombination of free and bound excitons. PL spectrum normally displays two emission bands (UV and broad emissions) under ambient conditions [144], [145], [146], [147], [148]. UV emission band is associated with a near band edge (NBE) transition of ZnO, which denotes the recombination of free excitons. In addition, a broad emission band is observed between 420 and 700 nm in almost all samples irrespective of the synthesis method and growth factors. This emission discernible in the visible region is referred to as deep level emission (DLE) which is attributable to defect formation and the presence of

impurities in the crystal structure such as O-vacancy, Zn-vacancy, O-interstitial, Zn-interstitial, and extrinsic impurities like substitutional Al. It has been reported that the green band emission evident in the region of 520 nm is indicative of the singly ionized oxygen vacancy in ZnO and is generated by the recombination of a photo-generated hole with the singly ionized charge state of this defect.

2.3 Review of Methods to Synthesize ZnO Nanostructures

There are many different methods of synthesis, both highly accurate by atomic deposition and by simple synthesis methods involving chemical reactions to make the nanostructure. There are many synthesis methods for preparing the ZnO nanostructures. It can be divided into the vapor and liquid-phase method. The example of the vapor phase method are vapor-liquid-solid (VLS), chemical vapor transport (CVT), thermal chemical vapor deposition, metal-organic vapor-phase-epitaxy (MOVPE), and metal-organic chemical vapor deposition (MOCVD) [11], [12], [13], [14], [149]. Examples of the liquid-phase method are chemical bath deposition, hydrothermal, wet oxidation, electrodeposition, and sol-gel [7], [15], [16], [84]. Compared to the vapor method, the liquid phase method is easier to handle.

2.3.1 Chemical Bath Deposition (CBD) Method

Chemical bath deposition also known as chemical solution deposition, liquid phase deposition, chemical deposition and aqueous solution method. It is a method of depositing thin film and nanomaterial in the solution phase. It was first reported in

1869 [150]. CBD generally entails the synthesis in solution, which involves oxide deposition and hydrolysis of metal cations which requires low growth temperature of < 300℃. It captured the researcher's interest due to the ability to change the properties of ZnO, producing a better orientation of crystallites, simpler method, works at low temperature, in a standard lab facility, and be applied at a wide scale [151]. Besides, CBD can coat many substrates in a single run [152] . Other methods such as molecular beam epitaxy, pulsed laser deposition, and chemical vapor deposition are complicated procedures, requiring expensive machines and are not environmentally friendly.

Many factors can affect CBD such as chemical bath solution pH, complexing agent, bath temperature, deposition time, concentration of cation and anion sources, type of precursor sources, ageing of the stock solution, and nature of substrates and their separation (separating the different phases of materials that are synthesized on a substrate) [152].

Numerous alternatives had been employed in order to synthesize the high-quality films and well oriented ZnO nanorod arrays. For example, incorporating a seed layer before the growth process. In [107], different thickness of ZnO seed layer have been deposited on Si substrate before CBD. It was found that an average diameter of ZnO NRs vertically deposited on the substrate was proximate to the average grain size of ZnO thin film. Other than that, work in [153] conclude that the crystal structure, morphology, and growth rate of the ZnO NRs was strongly dependent on the thickness and structure of the seed layer.

The ZnO has two polar and six non-polar surfaces as it is from the wurtzite crystal structure. The two polar surfaces are (0001) Zn terminate face and $(000\bar{1})$ O terminate face. The polar surface has higher surface energy than the non-polar surface

[154]. Therefore, during CBD the polar ZnO surface would attract opposite charges (Zn^{2+}) or (OH^{-}) from the solution to form ZnO nuclei. According to [155], annealing the seed layer before CBD growth can improve the reactivity of the seed-layer surface and result in a stronger electrostatic interaction between the polar surface and the ZnO nuclei in the solution. As a result, the annealed seed layer will attract more ZnO nuclei and lead to a higher growth rate.

The two-step CBD was proven to be the most effective approach for controlling size and alignment of the ZnO NRs [121]. Therefore, the two-step CBD technique with the incorporation of a seed layer was used in this work.

Two steps of CBD involve: heterogeneous nucleation and crystal growth. The heterogeneous nucleation is the deposition of aqueous ions onto a solid substrate to form homogenous thin films. The CBD starts with depositing the ZnO seed layer on the substrate. The deposition can be done using RF sputtering [156], thermal deposition [157] and spin coating [158]. In this work, seed layer deposition takes place using radio frequency (RF) sputtering on the glass substrate. For growing ZnO nanostructure, the seed layer is not necessary. However, the ZnO nanorods grown from the seed layer were able to grow at [0001] orientation, forming good crystal quality, uniform dissolution of nanorods, increasing the growth rate, and have optimal nucleation [159], [160]. Therefore, a ZnO seed layer was used in this work. To note, the seed layer with higher coverage density of the active nucleation sites, optimized thickness, and low surface roughness is important to obtain a higher aspect ratio and higher density of well-oriented ZnO nanorods [161], [162].

In this work, zinc nitrate and hexamethylenetetramine (HMT) were diluted to synthesise the ZnO nanorods, using CBD method. HMT is a base and acts as a pH

controller for the solution's pH is between six and seven to supply enough hydroxyl (OH) ions.

2.3.2 Hydrothermal

ZnO nanostructures can be grown using the hydrothermal method. It offers a cheap, simple setup, environment friendly low-temperature experiment. But still, it required a closed system and high vapour pressure condition [163], [164], [165]. For hydrothermal synthesis process, water is used as a solvent because it is a polar solvent due to the bent shape of water molecules. The polarity of water makes it capable to attract either negative or positive charges of an atom. Note that, the polarity of water could be modified by changing the temperature and pressure [166] .

There are two main steps of hydrothermal: seeding of the seed layer and growing of nanostructure. For growing the ZnO nanostructure's step, the seed layer is not required but it gives effect on nanostructure in term of shape and alignment [167]. For seeding step, many techniques can be employed such as sputtering, chemical spray pyrolysis (CSP) technique and seeding solution [168]. Commonly, the seeding solution is a mixture of zinc acetate and other solutions [164], [168], [169], [170], [171]. During hydrothermal growing process, it involves submerge of substrate in growth solution which is a mixture zinc nitrate and hexamethylenetetramine (HMTA) [170], [171]. The substrate is then rinsed with distilled water, dried with nitrogen gas and annealed. Based on works in [168], it was found that the best growth duration under hydrothermal method for highest density of nanorods is 10 hours. It also reveals that the growth duration did affect the length of ZnO nanorods.

2.3.3 Wet Oxidation

ZnO nanostructures such as nanowires, nanobelts and nanorods has been successfully synthesized by using wet oxidation technique [172], [173]. The setup and parameters such as temperature and pressure may vary, but the method does exhibit a common element which is water vapor. Thus, the name wet oxidation. The wet oxidation offers low cost, simple to fabricate, environment friendly and catalyst-free [174], [175]. Besides, it was found in works [172], [175], the nanostructure grown by wet oxidation have a strong adhesion to the substrate. The temperature during oxidation and wet oxidation time, two parameters that affects the grown nanostructure [175]. Wet oxidation is preferred instead of dry oxidation because wet oxidation ensures a non-planar growth of ZnO [175]. It was found in [173], the growth of ZnO nanostructures is in fact affected by water vapor. Furthermore, according to [176], the amount of water vapor in the environment will affect the PL luminescence and resistivity of the oxide formed.

2.4 Metal-doped ZnO

In semiconductors, doping can be defined as introducing impurities into extrinsic elements to improve and alter their basic properties such as structural, optical, and electrical [17] . However, doping can be critical to improve and tune its crystal structure due to low carrier concentrations and low resistance value [177]. With respect to n-type doping the natural background is still an issue. It is especially difficult to